

Model calculations of local electron and phonon densities of states in bimetallic superlattices

Madhu Menon and Gerald B. Arnold

University of Notre Dame, Notre Dame, Indiana 46556

(Received 8 November 1982)

We have analytically obtained the exact Green's functions for electrons and phonons in a bimetallic superlattice. The electrons are treated in the tight-binding approximation, and the phonons are of one acoustic branch in a lattice with nearest-neighbor coupling. The most interesting effects arise near the interfaces when the acoustical or electronic coupling between layers is large compared to the intralayer coupling. In this large coupling case, the local phonon density of states at low frequency is enhanced by a linear contribution due to interface modes. The appearance of electronic interface states in the local density of states is discussed. The impact of our results on superconducting properties is considered. The influence of zone-folding effects is found to be small.

I. INTRODUCTION

Recently there has been great interest in the fabrication and measurements of properties of bimetallic superlattices. Schuller and Falco¹ have made Nb-Cu layered ultrathin coherent structures which are superconducting. Durbin *et al.*² have also made high-quality Nb-Ta superlattices. Geerk *et al.*³ have made superconducting Nb-Al and Nb-Ta superlattice structures, as well.

In this paper, we shall explore the influence of superlattice and interface effects on the local density of states (LDOS) for electrons and the LDOS for phonons in a bimetallic superlattice. The locality of the screened electron-phonon interaction and the screened Coulomb interaction in a metal will cause these local densities of states to be significant in the determination of superconducting properties of these superlattices. We find that a great deal of interesting qualitative effects can be extracted by considering simple models. The superconducting properties of bimetallic superlattices will be further considered in a separate paper.⁴

Previously, we have presented results on the LDOS for phonons in a thin metal film backed by a semi-infinite metal.⁵ We have also considered the transmission coefficient of a single metal-metal interface for phonons⁵ and for electrons,⁶ using the Green's-function method.

The Green's-function method has played an important role in the study of surface and interface states. There have been a number of contributions to this field.

A Green's-function theory of surface states was

developed by Kalkstein and Soven.⁷ Starting from the energy eigenvalues of an infinite crystal, they generated the Green's function of a semi-infinite crystal using standard techniques. They also included the effect of attenuation in the surface potential. With the aid of this Green's function they calculated various local and total densities of states for surface states. An extension of their technique has been used by Yaniv⁸ to investigate the local density of states at a metal-metal interface. Varea and Robledo⁹ have developed a surface electronic Green's function in terms of the bulk Green's function via random walk theory, a different approach which has the same result as in Ref. 7.

A surface breaks the translational invariance along the direction perpendicular to it. One can still take advantage of the unbroken symmetry along the other two directions, however, and use Bloch's theorem.¹⁰ In Ref. 10, Kohn takes the crystal potential as spherical in the atomic spheres and as dependent only on the coordinate normal to the film in the region just outside the bounding atom planes.

In his paper on the calculation of the surface density of states, Kolar¹¹ has presented a derivation of a closed formula which gives the surface density of states of a semi-infinite tight-binding crystal in terms of the Green's function of the corresponding perfect (infinite) crystal. He has later used his formulation to treat more complex tight-binding systems.¹² A surface Green's function for N interfaces has been investigated by Bartos,¹³ N being finite, while Lee and Joannopoulos¹⁴ have used the transfer-matrix approach in the study of electronic surface states.

Our work differs from the above authors in that we use the Green's-function theory to investigate the local densities of states at the interfaces of a superlattice formed by repeating a double-layer film of metals (a and b) an infinite number of times. Various limits such as that of a thin film and bulk (infinite) systems are obtained by a simple choice of the coupling parameters. The formalism developed can be used both for phonons, and, with some modification, for electrons. Our final approach is similar to that of Kalkstein and Soven.⁷

The lattices of metals a and b are both assumed to be simple cubic with the same spacings. In addition, only nearest-neighbor coupled phonons and tight-binding electrons are considered. For simplicity we specialize at the beginning to the case of a single s band for electrons and acoustic branch for phonons. These assumptions allow us to obtain an exact solution to the problem of finding the Green's function. The results of numerical computations are presented.

Section II deals with the formalism. In Sec. III it is shown how we can use the formalism to treat phonons and electrons. The meaning of quasi-one-dimensional subbands is explained in detail in this section. Sections IV A and IV B deal with results and interpretations. In Sec. V we discuss the relevance of our results to superconducting properties, and in Sec. VI we summarize our conclusions.

II. FORMALISM

We shall consider thin films of metals a and b having atoms which are coupled by spring constants K_a and K_b , with atomic masses M_a and M_b . Simple manipulations of the equations of motion for lattice vibrations show that the relevant dynamical matrix involves the ratio of the spring constant to the mass $T_{a,b} = K_{a,b}/M_{a,b}$ as the fundamental parameter. If the spring constant for springs coupling a layer of metal a to one of metal b is defined as K , then the relevant coupling parameter which appears in the dynamical matrix is $T = K/(M_a M_b)^{1/2}$. Written in terms of $T_{a,b}$ and T , the equations of motion for vibrations in simple cubic lattices with only nearest-neighbor coupling in the presence of interfaces normal to the [100] direction (for example), are readily seen to be identical in form to the equation of motion for tight-binding electrons in the same system. In the electron case, $T_{a,b}$ and T are interpreted as interatomic nearest-neighbor overlap integrals, and ω^2 is replaced by the energy E . This mathematical correspondence will be exploited below to calculate the electron and phonon Green's function for isolated thin films of metals a and b , an isolated double layer of metal a and metal b , and a superlat-

tice of these two metals. We shall focus primarily on the superlattice results.

The superlattice considered in this paper is formed as follows. Thin films of metals a and b with effective spring constants (or, for electrons, overlap integrals) T_a and T_b , respectively, are coupled together, with T being the effective spring constant (overlap integral) for this coupling.

Coupling here constitutes a perturbation. This system of coupled films is then repeated an infinite number of times. See Fig. 1. The periodicity generated thereby allows use of Bloch's theorem in obtaining the Green's function for the superlattice from the Green's function of an isolated double-layer film.

The superlattice Green's function is obtained in stages as follows. First, we construct the isolated thin-film Green's function from the bulk Green's function.

The bulk Green's function is given by (Ref. 7)

$$G_0(n) = \frac{+i}{(4T^2 - \psi'^2)^{1/2}} \times \left[\frac{\psi' - i(4T^2 - \psi'^2)^{1/2}}{2T} \right]^{|n|}, \quad (2.1a)$$

where for phonons

$$\psi' = \omega^2 - \omega_0^2 [3 - \cos(k_y d) - \cos(k_z d)], \quad (2.1b)$$

$$2T = \omega_0^2, \quad (2.1c)$$

and for electrons

$$\psi' = E - 2T [3 - \cos(k_y d) - \cos(k_z d)], \quad (2.1d)$$

$$T = \langle n, k_{||} | H | n \pm 1, k_{||} \rangle, \quad (2.1e)$$

$$\vec{k}_{||} = (k_y, k_z),$$

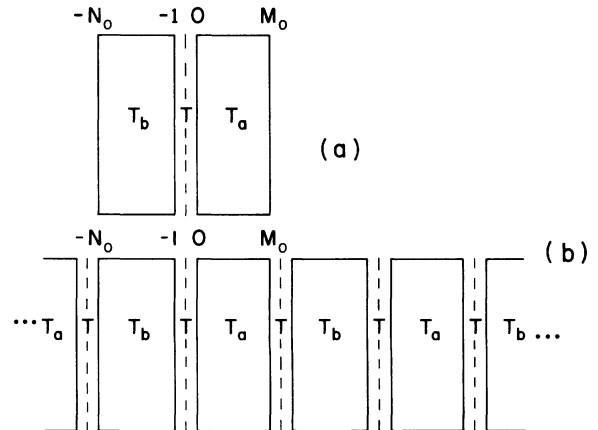


FIG. 1. (a) Double layer of metals a and b with intralayer couplings T_a and T_b , interlayer coupling T . (b) Double layer repeated infinitely to form a superlattice.

and d in both cases is the lattice spacing. Equation (2.1a) is obtained after performing an integration over k_x . Also, $k_{||}$ here means parallel to the $y-z$ plane. For simplicity, we have neglected site-diagonal perturbations.

If $\psi'^2 > 4T^2$ the square root must be interpreted as

$$i \operatorname{sgn}(\psi')(\psi'^2 - 4T^2)^{1/2}.$$

Equation (2.1a) can be written more simply as

$$G_0(n) = \frac{i}{\mu} \exp(i |n| \theta), \quad (2.2a)$$

where

$$\tan \theta = \frac{-(4T^2 - \psi'^2)^{1/2}}{\psi'} \quad (2.2b)$$

and

$$\mu = (4T^2 - \psi'^2)^{1/2} = 2T \sin \theta = \omega_0^2 \sin \theta. \quad (2.2c)$$

We then form a thin film by inserting two cleavage planes, the planes being between layers $-1, 0$ and M_0 and $M_0 + 1$. These two cleavage planes isolate the thin film from the bulk.

Let H_0 and H_t be the Hamiltonian for the bulk and the thin film, respectively, and G_0 and G_t the corresponding Green's functions. We then have the operator equation

$$(E + i\delta - H_t)G_t = 1, \quad (2.3)$$

$$G_{2t}(M, M) = \frac{-1}{T_a} \frac{\sin[(M_0 + 1 - M)\theta_a] \{ \sin[(M + 1)\theta_a] \sin[(N_0 + 1)\theta_b] - \gamma \sin(M\theta_a) \sin(N_0\theta_b) \}}{\sin\theta_a \{ \sin[(M_0 + 2)\theta_a] \sin[(N_0 + 1)\theta_b] - \gamma \sin[(M_0 + 1)\theta_a] \sin(N_0\theta_b) \}}, \quad (2.7a)$$

where

$$\theta_{a,b} = -\arctan(4T_{a,b}^2 - \psi'_{a,b})^{1/2} / \psi'_{a,b}, \quad (2.7b)$$

$$\gamma = \frac{T^2}{T_a T_b}. \quad (2.7c)$$

From Eq. (2.7b) we see that the tangent has an imaginary argument except when

$$\begin{aligned} -1 &\leq \frac{\psi'_a}{2T_a} \leq +1, \\ -\frac{T_b}{T_a} &\leq \frac{\psi'_b}{2T_a} \leq \frac{T_b}{T_a}. \end{aligned} \quad (2.8)$$

Hence the allowed (i.e., real) values of θ are given by this equation. Note also that

$$\operatorname{sgn}[\operatorname{Im}(\theta_{a,b})] = \operatorname{sgn}(\psi'_{a,b}). \quad (2.9)$$

We now move on to the superlattice case [see Fig. 1(b)]. The Green's function G for the superlattice is obtained in terms of G_{2t} and the perturbation T by

where E is the energy and δ a positive infinitesimal. G_t is given in terms of G_0 and the perturbation $T_t = H_t - H_0$ ($t = a$ or b) by the equation

$$G_t = G_0 + G_0 T_t G_t, \quad (2.4)$$

where T_t connects layers -1 and 0 and M_0 and $M_0 + 1$ only. The film is $M_0 + 1$ layers thick. G_t cannot connect any layer inside to any layer outside the thin film. The result for $M \geq 0$ is

$$G_t(M, M) = \frac{-1}{T} \frac{\sin[(M_0 + 1 - M)\theta] \sin[(M + 1)\theta]}{\sin\theta \sin[(M_0 + 2)\theta]}. \quad (2.5)$$

After having obtained the Green's function for a thin film G_t , we now couple two thin films of metals a and b , where the interface is formed between layers -1 and 0 [see Fig. 1(a)].

Film b is N_0 layers thick. To obtain the Green's function G_{2t} for the two-layer system, we again use Eq. (2.4) rewriting it as

$$G_{2t} = G_t + G_t T G_{2t} \quad (2.6)$$

and employ the fact that G_{2t} can now connect layers in a to those in b but G_t cannot. The perturbation T now connects layers -1 and 0 . The result for M in film a is

$$\begin{aligned} G(M, M) &= G_{2t}(M, M) + G_{2t}(M, M_0) T G(M_0 + 1, M) \\ &\quad + G_{2t}(M, -N_0) T G(-N_0, -1, M). \end{aligned} \quad (2.10)$$

The presence of periodicity in the system enables one to use Bloch's theorem which in the context of this problem states that G 's in different superlattice unit cells must be related by a phase factor. That is,

$$\begin{aligned} G(M_0 + 1, M) &= e^{-i\phi} G(-N_0, M), \\ G(-N_0 - 1, M) &= e^{i\phi} G(M_0, M), \end{aligned} \quad (2.11)$$

where

$$\phi = k_{\perp} (M_0 + N_0 + 1) d.$$

Using Eqs. (2.7), (2.10), and (2.11), and integrating over the phase ϕ from $-\pi$ to π , we get for $M_0 \geq M \geq 0$,

$$G(M, M) = -\frac{1}{T_a \sin \theta_a} \frac{\gamma(\gamma DE - AB) \sin[(M_0 - M)\theta_a] + A\alpha \sin[(M_0 + 1 - M)\theta_a]}{(a^2 - b^2)^{1/2}}, \quad (2.12)$$

where

$$\alpha = \sin[(M_0 + 2)\theta_a] \sin[(N_0 + 1)\theta_b] - \gamma \sin[(M_0 + 1)\theta_a] \sin(N_0\theta_b),$$

$$A = \sin[(M + 1)\theta_a] \sin[(N_0 + 1)\theta_b] - \gamma \sin(M\theta_a) \sin(N_0\theta_b),$$

$$B = \sin[(M_0 + 2)\theta_a] \sin(N_0\theta_b) - \gamma \sin[(M_0 + 1)\theta_a] \sin[(N_0 - 1)\theta_b],$$

$$C = \sin[(M_0 + 1)\theta_a] \sin[(N_0 + 1)\theta_b] - \gamma \sin(M_0\theta_a) \sin(N_0\theta_b),$$

$$D = \sin[(M_0 + 1 - M)\theta_a] \sin \theta_b,$$

$$E = \sin \theta_a \sin \theta_b,$$

$$a = \alpha^2 + [\gamma^2 E^2 - \gamma BC],$$

$$b = 2\gamma\alpha E.$$

One can check that Eq. (2.12) gives the right bulk limit when $T_a = T_b = T$, i.e., $\gamma = 1$. The result for one isolated thin film (a or b) is obtained when one puts $T = 0$ (i.e., $\gamma = 0$).

III. PHONONS AND ELECTRONS

The formalism developed can be used for both phonons and electrons. First let us consider phonons. We see from Eq. (2.8) that the allowed values of $\psi'_a/2T_a$ must lie between -1 and 1 for θ_a to be real. Indeed one can see from Eq. (2.2) that for high enough energies $G_0(n)$ falls off exponentially since $\text{Im}\theta_a > 0$ for $\psi'_a > 0$. Therefore, the LDOS must also fall off exponentially outside the range for which θ_a is real. On the other hand, Eq. (2.1b) yields, since $-\pi \leq k_y d, k_z d \leq \pi$,

$$\frac{\psi'_a}{2T_a} + 1 \leq \frac{\omega^2}{2T_a} \leq \frac{\psi'_a}{2T_a} + 5. \quad (3.1)$$

Combining (2.8) and (3.1) we see that

$$0 \leq \frac{\omega^2}{2T_a} \leq 6. \quad (3.2)$$

Equation (3.2) determines the range of frequencies allowed in metal a , taking into account all possible k_y, k_z values. Similarly from Eqs. (2.8) and (2.1b) one can easily show that in metal b ,

$$0 \leq \frac{\omega^2}{2T_a} \leq \left[6 \frac{T_b}{T_a} \right]. \quad (3.3)$$

This defines the range of frequencies allowed in metal b . These frequency ranges define the regions over which the local phonon density of states is expected to be nonvanishing in bulk metal a or metal b .

For electrons one is concerned with energy rather than frequency [see Eq. (2.1d)]. Furthermore, one

has to consider the Fermi level for electrons. When two metals are brought into contact the Fermi levels become aligned. Since the positions of Fermi levels in metals depend upon the filling of the bands and the bandwidths are in general different, the bottoms (and tops) of the allowed energy ranges for the metals in contact do not necessarily coincide. One can conveniently choose the zero of energy to be halfway between the bottoms of the allowed energy ranges for metals a and b and define a parameter V , where $2V$ is the Fermi-energy difference.

To take into account all these things we rewrite Eq. (2.1d) as

$$\begin{aligned} \psi'_a &= E - 2T_a [3 - \cos(k_y d) - \cos(k_z d)] + V, \\ \psi'_b &= E - 2T_b [3 - \cos(k_y d) - \cos(k_z d)] - V. \end{aligned} \quad (3.4)$$

Again one can show that the range of allowed energies in metal a , taking into account all possible k_y, k_z values, has a width

$$-\frac{V}{2T_a} \leq \frac{E}{2T_a} \leq 6 - \frac{V}{2T_a}, \quad (3.5a)$$

and in metal b ,

$$+\frac{V}{2T_a} \leq \frac{E}{2T_a} \leq 6 \frac{T_b}{T_a} + \frac{V}{2T_a}. \quad (3.5b)$$

In all the plots for electrons, we have plotted $E/2T_a$ on the horizontal axis. We have assumed that the metals a and b are "good" metals, i.e., "band bending" is absent near the junction. This is a reasonable approximation since electrons in metals efficiently screen any electric field so that, to an excellent approximation, the band edges change abruptly at the interface, like a step function.

A useful framework for discussing many interface phenomena is provided by the notation of "subbands" for the two metals. A subband is a quasi-one-dimensional band obtained by determining the maximum range of frequency (phonons) or energy (electrons) for which nonexponentially decaying states are found in a given metal at some fixed set of wave-vector values (k_y and k_z). Since the subbands are defined at a fixed set of wave vectors, the frequency and energy ranges are different from those discussed above, where all possible wave vectors were taken into account.

For example, one finds propagating states in metals a and b when θ_a and θ_b are real. From (2.2c) one has

$$\sin\theta_a = [1 - (y - x_+)^2]^{1/2} \sin\theta_b = [1 - (y - Rx_-)^2]^{1/2},$$

where

$$x_{\pm} = \begin{cases} \frac{\omega^2}{2T_a} & \text{(phonons)} \\ \frac{E \pm V}{2T_a} & \text{(electrons)} \end{cases}$$

and

$$y = 3 - \cos(k_y d) - \cos(k_z d),$$

$$R = T_a/T_b.$$

For each value of y there is a distinct pair of subbands, one on each side of the interface, comprising a subband configuration (cf. Fig. 2). The metal a subband is the range of x_+ values given by

$$y - 1 \leq x_+ \leq y + 1$$

and the metal b subband is defined by the range

$$\frac{1}{R}(y - 1) \leq x_- \leq \frac{1}{R}(y + 1).$$

It is convenient to choose the subband configuration at normal incidence ($k_y = k_z = 0$, i.e., $y = 1$) as a "fiducial" configuration. For phonons, the bottoms of metal a and metal b subbands coincide for $y = 1$. For electrons, a nonzero Fermi-energy difference ($2V \neq 0$) causes the subband bottoms to be displaced from one another for $y \neq 1$.

As the angle of incidence increases (i.e., y in-

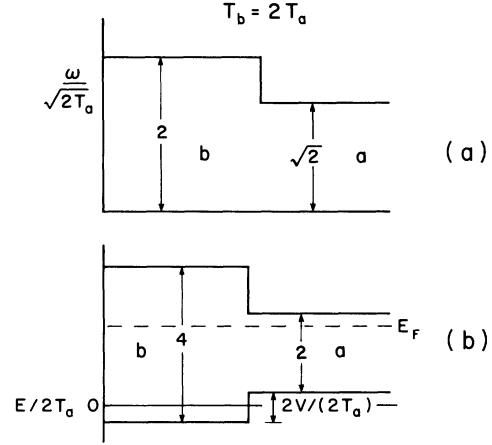


FIG. 2. (a) Subband diagram for phonons in metals a and b , when $T_b = 2T_a$. (b) Subband diagram for electrons in metals a and b , for $T_b = 2T_a$. V is half the difference between Fermi energies of a and b .

creases) the subbands of metal a and metal b are rigidly shifted upwards. If R is different from unity, then the amount by which each subband is shifted will differ. For example, if $R = 2$, the metal a subband will shift up twice as far as the metal b subband with increasing y . For $R > 1$, if there exists a y value such that

$$y - 1 - V/2T_a = \frac{1}{R}(y + 1 + V/2T_a)$$

then, at this value, the bottom of the metal a subband may coincide with the top of the metal b subband. For larger y values (increasing angle of incidence) there is no transmission through the interface⁶ regardless of the value of the intermetallic coupling, T . It is clear from the subband configuration at this critical y value that it is no longer possible to pass from a propagating state in metal a to one in metal b (or vice versa). The subband picture is clearly an ideal one for discussing the wave-vector dependence of interface phenomena.

IV. RESULTS

In this section, we shall present our results for the local density of states for the M th metal a layer of a superlattice. The quantity we have calculated is

$$\rho(x, M) = -\frac{D}{\pi} \sum_{k_y, k_z} \text{Im}G(M, M; x; k_y, k_z). \quad (4.1)$$

For electrons $x = E$, $D = 1$, and for phonons $x = \omega^2$, $D = 2\omega/(2T_a)^{1/2}$. The Green's function in (4.1) is given by (2.12).

A. Phonons

The local density of states is plotted as a function of frequency [frequency has been normalized to $(2T_a)^{1/2}$, the metal a subband width, and is therefore dimensionless in our units]. Variations in the LDOS are observed as a function of coupling spring constant T and layer index M . The layer integers M_0 and N_0 are each taken to be 5. Also, to simplify the numerical calculations, a small constant imaginary number (0.01) was added to the phonon frequency, ω . In all cases, the total area under the LDOS curve was checked and found to be within 0.5% of unity, in reasonable agreement with the sum rule.

Figure 3 illustrates the dependence on T of the extra contributions to the LDOS at high and low frequencies. Recall that T is the ratio of the spring constant K for springs linking a - and b -metal planes at the interface, divided by the geometric mean of the a - and b -metal atomic masses. As T increases, the mechanical coupling grows, and one finds an increasing density of modes at low frequency, for one expects the coupling at first to eliminate the geometric cutoff at low q , and then gradually to allow for more and more low- q phonons as it increases. One might intuitively expect the density of low- q (low- ω) modes to saturate at its bulk value, but this is *not* the case (cf. inset, Fig. 3).

Figure 4 illustrates that the enhancement of the low-frequency LDOS by increasing T is a local, inter-

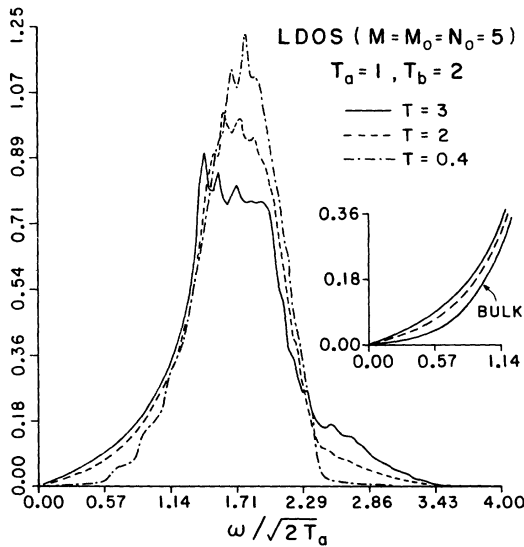


FIG. 3. Local phonon density of states at the interface, in metal a of a superlattice for various interlayer coupling, T . The inset is the low-frequency portion of the large curve, except that the dashed-dotted curve is replaced by the *bulk* a metal result.

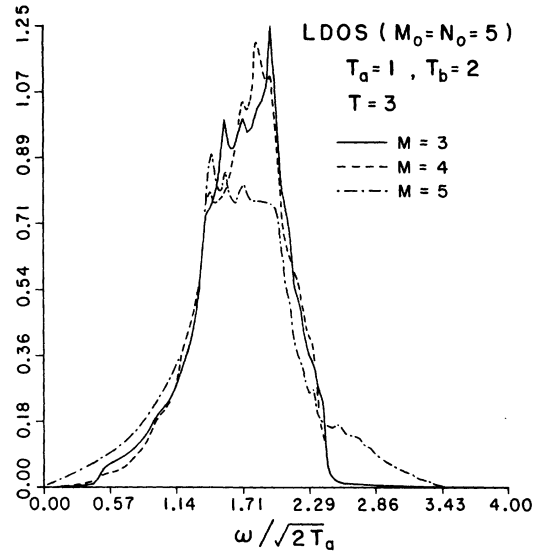


FIG. 4. Local phonon density of states in metal a of a superlattice for large interlayer coupling T at the interface ($M=5$) and one and two layers into metal a from the interface.

face phenomenon, which disappears as one evaluates the LDOS farther from the interface. Consistent with the nearest-neighbor coupling approximation, the effect is observed only at the interface ($M=5$). It is remarkable that increasing the stiffness of the springs connecting two metal films in a superlattice (i.e., increasing T) should result in an increase in the density of modes at low frequency for both metal films at the interface. A physical explanation of the origin of this low-frequency LDOS enhancement is best provided by making use of the analogy between tight-binding electrons and nearest-neighbor coupled phonons. We shall therefore defer the explanation to discussion of the electron case.

A similar enhancement of the LDOS is seen in Fig. 3 for high frequencies as T increases. In this case it is easy to see that this arises from the fact that the metal across the interface (metal b) has a larger phonon subband bandwidth (by a factor of $\sqrt{2}$). There is, in essence, a “leaking” of modes from metal b at frequencies which are forbidden in bulk metal a [cf. the subband configuration in Fig. 2(a)]. Hence the stronger mechanical coupling to the metal b allows excitation of vibrational modes at frequencies which would be forbidden in bulk metal a . The exponential attenuation of these modes in the metal a (cf. Fig. 4) causes the enhancement to be a local phenomenon.

The superlattice periodicity is expected to yield “zone-folding” effects. The influence of these on the LDOS are very subtle, however, because of the three dimensionality of the system, which smears

out the Van Hove singularities which arise from the superlattice periodicity. In Fig. 5 we compare the superlattice LDOS one layer in from the interface with the bulk LDOS and the LDOS for an isolated double layer. The superlattice periodicity does modulate the isolated double layer LDOS to some extent, but the effects are not dramatic. Incidentally, we plot these LDOS's at a layer away from the interface because at the interface, the interface mode phenomena discussed above obscure the superlattice effects.

It is instructive to investigate the effects of three dimensionality on the LDOS. These effects are generated by the $k_{||}$ $[=(k_y^2 + k_z^2)^{1/2}]$ dependence of (2.12), which appears as y dependence of the subband configuration. As y increases from unity (the normal incidence value) both subbands shift their bottoms upward, above $\omega=0$. We therefore conclude that *low* values of $k_{||}$ are most important at low frequencies. In order to attain the upper end of the range of allowed frequencies (near $\omega^2/2T_a=6$), it is clear that *large* $k_{||}$ values (i.e., y near 5) are required in order to shift the subbands up to this frequency region. Hence at high frequencies large $k_{||}$ values are most important.

One may infer from these observations that the one-dimensional aspects of the superlattice dominate at low ω , while more local features should be emphasized at high ω . Further, these facts imply that the roughness of the interface has a greater influence on the low-frequency behavior, because such roughness has its largest effect on waves traveling normal to the interface ($k_{||} \approx 0$). The high-frequency

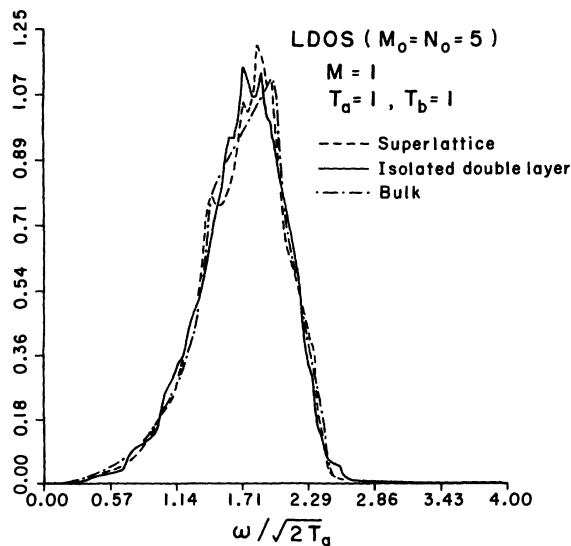


FIG. 5. Local phonon density of states in metal a one layer away from the interface for a superlattice compared to same for an isolated double layer, and to bulk a metal.

behavior should be less sensitive to surface roughness, because waves which travel at glancing angles to the interface are least affected by this roughness.

B. Electrons

For electrons the LDOS's are plotted as a function of energy (energy has been normalized to $2T_a$, the metal a subband width, and therefore is dimensionless in our units). Unlike phonons, the bottoms of the a and b subbands do not coincide for normal incidence (cf. Sec. III for a detailed discussion on subbands). Instead Fermi levels in both metals must align when brought in contact. We chose the zero of energy to be halfway between the bottoms of the a and b subbands at normal incidence. In Figs. 6(a) and 6(b) we display normal incidence subbands for two different choices of parameters.

In the numerical results presented below, the layer integers were again chosen to be $M_0=N_0=5$ and the numerical calculations were performed with a small constant imaginary number (0.01) added to the electron energy E .

In Fig. 7, we plot the LDOS at the interface in metal a for the situation represented in Fig. 6(b). For $T=0$ one has the LDOS at the surface of an isolated metal a film. As T increases one notes the appearance of interface states in the LDOS at both ends of the subband, and a downward shift of peak energies, as in the phonon case.

These interface states are located at energies which are forbidden in the subbands of bulk metal a , but allowed in those of bulk metal b . The origin of these states is simply the leaking phenomenon described previously for the phonon case. The extent of the leakage effect increases as the intermetallic coupling T increases. These states were discussed by Yaniv⁸ who showed that they are confined to the interface layer, but freely propagating parallel to the interface. These leakage states are thus two dimensional in character.

Figure 8 illustrates the rapid attenuation of these

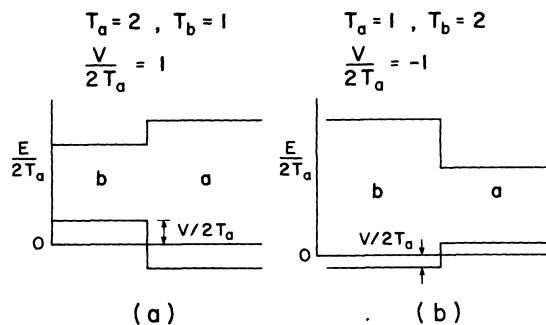


FIG. 6. Subband diagrams for electrons in two situations.

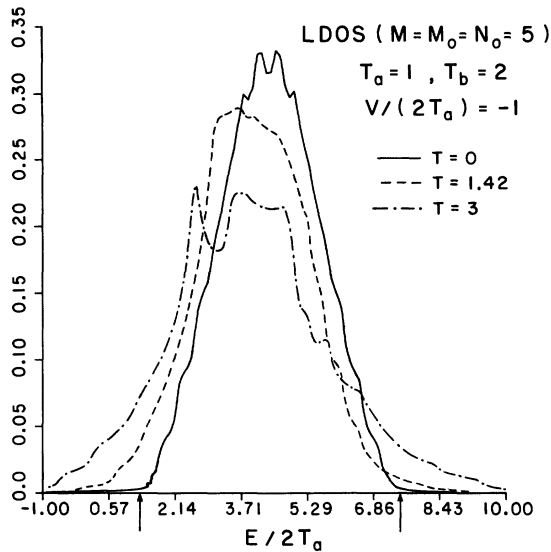


FIG. 7. Local electron density of states in metal a of a superlattice, evaluated at the interface for various interlayer coupling strengths. Vertical arrows along the abscissa indicate the bulk subband edges.

interface state contributions to the LDOS as one moves into the metal a . The asymmetry seen in the interface LDOS in Fig. 8 may be understood by referring to Fig. 6(b) and noting that the increased energy range and amplitude of interface state contributions to the LDOS correlates with the presence and relative location of the metal b subband at nor-

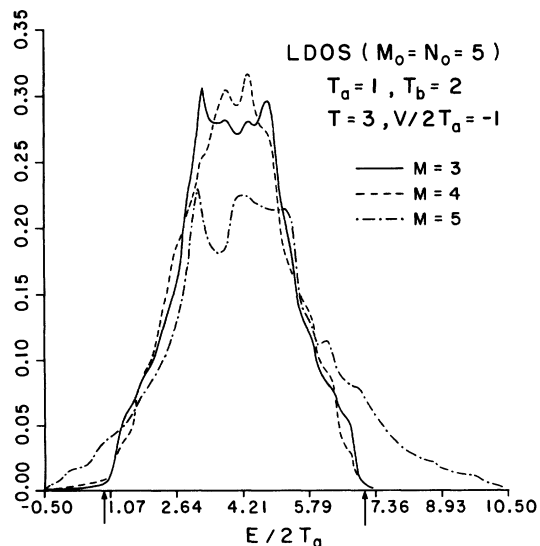


FIG. 8. Local electron density of states in metal a of a superlattice for strong interlayer coupling T evaluated at the interface ($M=5$) and at successive layers into metal a , away from the interface. Vertical arrows along the abscissa indicate bulk subband edges.

mal incidence. In Figs. 7 and 8 the bulk allowed range of metal a energies would extend between the two arrows along the $E/2T_a$ axis. The relatively strong electronic interface coupling T significantly extends the range of allowed states at the interface. To satisfy the sum rule, this means that the interface electronic density of states in the middle of the subband is depressed from its bulk value.

In Fig. 9 we consider the effect of variation in V (equal to one-half the difference between Fermi energies) on the LDOS for $T=2$, and equal a - and b -metal subband widths. The result for $V=0$ shows some interesting deviations from the bulk case ($T=1$), in that the subband width appears to have been broadened (the arrows along the horizontal axis locate the bulk subband edges) due to the presence of an overlap integral which is locally larger than for the neighboring layers. Also, two sharp peaks appear, symmetrical about the center of the LDOS. This is a local, *interface* phenomenon which also appears in the isolated double-layer system and in the two semi-infinite double-layer system having the same parameters. It is not a result of superlattice symmetry, because it is independent of the values of M_0 and N_0 . This effect is a consequence of the contribution of interface states arising from strong intermetallic coupling (T) in the LDOS at the interface. Yaniv⁸ has discussed such states for the case of two semi-infinite metal layers. As far as the interface states are concerned, the same discussion may be applied to the superlattice case, because

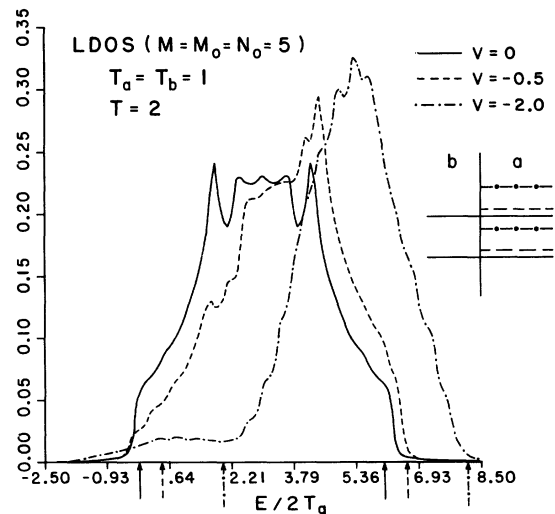


FIG. 9. Local electron density of states in metal a of a superlattice, evaluated at the interface for various Fermi energy differences, V . The relative subband orientations for metals a and b are depicted in the inset. The vertical arrows along the abscissa delineate the subband edges which would obtain for bulk a metal.

these states are localized in the interface planes. The interface states are two dimensional in character because they may freely propagate parallel to the interface.⁸

Such states will therefore contribute a two-dimensional density-of-states component to the LDOS at the interface. This two-dimensional component exhibits two logarithmic singularities symmetrically placed about the subband center (in our case, a small constant imaginary part added to the energy obliterates the weak singularities, leaving only sharp peaks) and falls smoothly to a nonzero constant at the band edges, dropping discontinuously to zero there. In Fig. 9 one can clearly discern the contribution of these large- T interface states to the LDOS. The phonon LDOS at the interface (cf. Sec. IV A) shows analogous effects for large T . One can now explain the extra density of modes at low frequency as arising from two-dimensional interface modes. At low frequency, the two-dimensional component of the LDOS varies *linearly* with frequency, adding to the quadratic frequency variation arising from the bulklike modes, so that as $\omega \rightarrow 0$, the LDOS varies linearly with ω . The implications of this for superconductivity will be discussed in Sec. V. As the concentration of interfaces in the superlattice increases, the LDOS at the interface will obviously become more influential in the average density of states for each film of the superlattice.

The asymmetry which develops in the electron LDOS as the magnitude of V is increased is shown in Fig. 9. For $V = -2$, there is a long, low-energy tail of states in the LDOS which arises from interface states of the leakage variety discussed above. The dependence of the LDOS on k_{\parallel} is completely analogous to that discussed in Sec. IV A for phonons.

We have also considered the effects of a site diagonal perturbation on electron states at the interface in both a and b metals. For large enough perturbation of this type, interface states are formed.⁸ The influence of these states upon the LDOS for electrons is qualitatively the same as discussed above for the large- T case because these states are also two-dimensional in character.

V. SUPERCONDUCTING PROPERTIES

Within our model we can calculate those one-electron and phonon properties which are relevant to superconductivity in each of the metal layers. Of primary importance is the local electron-phonon interaction (EPI) coupling parameter⁵ for the N th layer, analogous to the bulk McMillan parameter (λ) (Ref. 15):

$$\lambda_N = 2 \int_0^{\infty} d\omega \alpha^2(\omega, N) F(\omega, N) / \omega = \frac{\rho(E_F, N)}{M} \frac{I^2}{\langle \omega^2 \rangle_N}, \quad (5.1)$$

where $\alpha^2(\omega, N)$ is the local value of a convolution of the electron LDOS near the Fermi surface and an EPI matrix element. The phonon LDOS is $F(\omega, N)$, and the electron LDOS at the Fermi energy is $\rho(E_F, N)$. The average EPI matrix element connecting pairs of electron-hole states near the Fermi surface is designated by I , and M is the ion mass. The average squared frequency is defined by

$$\langle \omega^2 \rangle_N = 2 \int_0^{\infty} d\omega \omega \alpha^2(\omega, N) F(\omega, N) / \lambda_N.$$

In the following we shall assume that $\alpha^2(\omega, N)$ is independent of ω , so that the average $\langle \omega^2 \rangle_N$ depends only on phonon properties. The only quantity which we cannot calculate in our model is I . We shall henceforth assume that I has the same value in bulk samples, thin films, and superlattice films of a given metal. This approximation allows us to compare calculations of λ_N for bulk samples, thin films, and superlattice films of a given metal.

As noted in Sec. IV, differences between a thin film and a superlattice layer of metal a will only be apparent for strong intermetallic coupling T for electrons or phonons. Therefore, below we shall discuss the case for $T_a = 1$, $T_b = 2$, and $T = 3$ for phonons and electrons. We shall take $M_0 = N_0 = 5$ for the superlattice (i.e., 5×6 superlattice). In such a superlattice, the concentration of interfaces is 36%.

First, consider the electron LDOS. If there are interface states, then the LDOS at the edges of the allowed range of energies increases at the expense of the LDOS in the central portion of this range (because the LDOS must obey a sum rule). Assuming that E_F lies in this central portion, one concludes that electronic interface states have a *negative* influence on λ_N . If E_F lies in the upper or lower part of the allowed energy range, however, there will be a *positive* influence. The degree of these influences increases both as the intermetallic coupling T for electrons increases, and as the concentration of interfaces increases. In general, it seems that interface state formation will be undesirable from the point of view of improving superconducting properties.

In Fig. 10 we display the bulk densities of states and the single-film average DOS's (defined as the sum of the LDOS's for each layer divided by the number of layers in the film) for an isolated film and a superlattice film. The isolated film result seems to indicate a higher electron DOS than in bulk for the central range of allowed energies. The peaks arise from quantization size effects. However, had we included a surface perturbation, the isolated

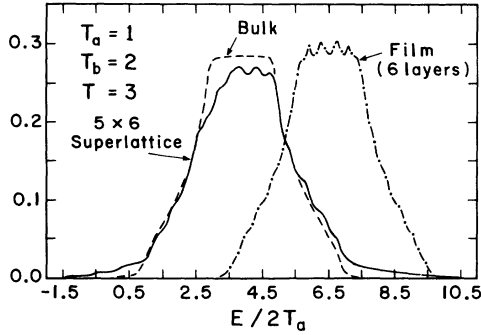


FIG. 10. Average electron densities of states in metal a for a bulk sample, a six-layer film, and a six-layer superlattice film.

film DOS would also fall below the bulk DOS for the central range, just as the superlattice film DOS does.

The contribution of phonons to the EPI coupling strength is contained in the factor $M\langle\omega^2\rangle_N$ of (5.1). Scaling all frequencies by $(2T_a)^{1/2}$, we find that in our model the local average is a ratio of two integrals. In Table I we present our results for these integrals and their ratio for three cases: the isolated film, bulk sample, and superlattice layer.

At the interface ($M=5$) in the six-layer metal a , the superlattice results indicate a 19% enhancement of λ_5 (due to the interface mode contribution at low ω) relative to the bulk EPI coupling value. When the average over six layers is computed, this enhancement is decreased to a value of 4%. Note that the isolated film results indicate that phonons in a film are less effective in producing superconductivity than are bulk phonons. The reason for this is obvious: In a film there is a maximum phonon wavelength, hence a minimum phonon frequency which is greater than zero. Because low-frequency phonons are important in superconduc-

tivity, the presence of a low-frequency cutoff for phonons will have a deleterious influence on the EPI coupling strength.

Naturally, the greater the concentration of interfaces (36% in the present example) the greater the influence of the enhancement. For the isolated film, the decrease in coupling strength will depend on the "concentration of surface," hence will become more prominent with decreasing film thickness.

We conclude that, in general, the superconductivity of films should worsen with decreasing film thickness, and the T_c of a film should be less than the bulk T_c , decreasing with decreasing film thickness. However, exceptions can occur if the Fermi energy happens to fall near a band edge, where surface states can increase the LDOS above that for a bulk sample, and cause T_c to increase with decreasing film thickness. In the latter case, the favorable electronic effects would still have to overcome the unfavorable phonon effect arising from the low-frequency cutoff in the film.

For superlattices, the only unequivocal statement which can be made about the superconductivity is that in any given layer the coupling will be larger than that of an isolated film of the same thickness. The reason this is so is that the generally unfavorable electronic effects are partially compensated by the favorable phonon effects which arise from interface modes and the absence of a low-frequency cutoff. If the bulk coupling is to be improved in a superlattice layer, the ideal situation is one in which the Fermi energy falls near one of the band edges, where interface state formation can increase the LDOS, and strong intermetallic phonon coupling T produces interface modes. Alternatively, one might seek a system in which electronic interface states are negligible but phonon interface modes are plentiful.

There is experimental evidence from Nb-Cu superlattices¹⁶ which indicates that a superlattice layer

TABLE I. EPI parameters.

| $A = \int dz F(z, M)/z$ | M | $B = \int dz zF(z, M)$ | $z = \omega/(2T_a)^{1/2}$ | $B/A = \langle z^2 \rangle_M$ |
|-------------------------|-----|------------------------|---------------------------|-------------------------------|
| Sample | | A | B | B/A |
| Superlattice layer | 5 | 0.694 | 2.393 | 3.448 |
| | 4 | 0.637 | 2.682 | 4.210 |
| | 3 | 0.640 | 2.679 | 4.186 |
| | av. | 0.657 | 2.585 | 3.948 |
| Film | 5 | 0.642 | 2.658 | 4.140 |
| | 4 | 0.640 | 2.670 | 4.172 |
| | 3 | 0.624 | 2.756 | 4.417 |
| | av. | 0.635 | 2.695 | 4.243 |
| Bulk | | 0.645 | 2.651 | 4.110 |

of Nb does indeed have stronger EPI coupling than an isolated Nb film of the same thickness. Since the EPI coupling in the Nb superlattice layer is less than the bulk coupling, and decreases with decreasing layer thickness (though not as rapidly as the isolated Nb film coupling decreases), it is evident that the unfavorable electronic effects are dominating the favorable phonon effects in the Nb-Cu superlattice.

VI. CONCLUSIONS

We have obtained an analytic expression for the Green's function of a metal-metal superlattice. This function describes the behavior of nearest-neighbor coupled phonons or tight-binding electrons in a superlattice. Because this is a relatively crude model of a superlattice, we have concentrated primarily on the qualitative features of the model. We believe that these features will be evident even in a more detailed theory.

The briefest possible summary of our results from the LDOS calculations for both electrons and phonons can be given as follows: The most dramatic and dominant effects in a superlattice arise at the interfaces, are local, interface phenomena, and are effects which require strongly coupled layers (large T). For smaller T values, the interface phenomena de-

crease in influence, and the LDOS approaches that of a *single* isolated layer.

To study superlattices which differ most from simple composites, one should endeavor to make both metal layers as thin as possible in order to obtain a high concentration of interfaces, so that the interesting interface phenomena will dominate. In the simple model presented here, this would require films of only one or two layers. However, realistically, the influence of interface states should extend over the range of electronic overlap, or, for phonons, the range of interatomic coupling. These ranges will certainly be longer than the single lattice constant range implicit in the approximate models employed here. Hence nonbimetallic composite effects may become evident in superlattices with metal slabs consisting of several atomic layers. The qualitative effects should be as discussed above. We conclude that bimetallic superlattices should allow the study of the influence of interface phenomena on bulk properties.

ACKNOWLEDGMENT

This research was supported by the National Science Foundation (NSF) under Grant No. DMR-80-19739.

-
- ¹I. K. Schuller, Phys. Rev. Lett. **44**, 1597 (1980); I. K. Schuller and C. M. Falco, in *Inhomogeneous Superconductors—1979 (Berkeley Springs, WV)*, Proceedings of the Conference on Inhomogeneous Superconductors, edited by D. U. Gubser, T. L. Francavilla, S. A. Wolf, and J. R. Leibowitz (AIP, New York, 1979).
- ²S. M. Durbin, J. E. Cunningham, M. E. Mochel, and C. P. Flynn, J. Phys. F **11**, L223 (1981).
- ³J. Geerk, M. Gurvitch, G. Hertel, D. B. McWhan, and J. M. Rowell, in *Superconductivity in d- and f-Band Metals* (Kernforschungszentrum, Karlsruhe, in press).
- ⁴G. B. Arnold, W. J. Gallagher, and E. L. Wolf, in *Superconductivity in d- and f-Band Metals*, Ref. 3.
- ⁵G. B. Arnold and M. Menon, J. Phys. (Paris) Colloq. **42**, C6-377 (1981).
- ⁶G. B. Arnold, Phys. Rev. B **25**, 5998 (1982).
- ⁷D. Kalkstein and P. Soven, Surf. Sci. **26**, 85 (1971).
- ⁸A. Yaniv, Phys. Rev. B **17**, 3904 (1978).
- ⁹C. Verea and A. Robledo, Phys. Rev. B **19**, 1310 (1979).
- ¹⁰W. Kohn, Phys. Rev. B **11**, 3756 (1975).
- ¹¹M. Kolar, Phys. Status Solidi B **83**, 625 (1977).
- ¹²M. Kolar, Phys. Status Solidi B **96**, 447 (1979).
- ¹³I. Bartos, Phys. Status Solidi B **85**, K127 (1978).
- ¹⁴D. H. Lee and J. D. Joannopoulos, J. Vac. Sci. Technol. **19**, 355 (1981).
- ¹⁵E. L. McMillan, Phys. Rev. **167**, 331 (1968).
- ¹⁶C. M. Falco and I. K. Schuller, in *Superconductivity in d- and f-Band Metals*, Ref. 3.